T. Bohl, BE/RF
2012-04-05
Internal Use Only

200 MHz beam component of the proton LHC beam in the SPS

Measurements during the scrubbing run 2012-03-26 to 2012-03-30

1 Introduction

During the SPS scrubbing run the wall current monitor WC-2 AEW.31731 together with the Agilent Signal Analyzer EXA N9010A was used to acquire the 200 MHz component of the beam current, I_{200}, versus time with a RBW of 3 MHz at the revolution period time scale and triggered at f_{rev}. Further details about the acquisition details and the movies made using these acquisitions can be found in App. A. The aim was to measure uncaptured beam. This had been done earlier in a similar way [1], [2], or using an oscilloscope [3].

2 2012-03-26

The cycle MD_26_L25200_2012x_V1 (ID: 1796), Timing User LHCMD1, MMI Target LHCMD1, (standard SPS optics, $\gamma_{\mathrm{t}} = 22.8$, 22 166 ms long flat bottom, no acceleration ramp) was used. The RF voltage programme consisted of segments of 2 MV (RF voltage dips) at the time of each injection (six injections), spaced 3.6 s, and was otherwise 3 MV. The 800 MHz RF system was programmed for a const. value of 350 kV. Typical bunch intensity $N_{\mathrm{Q}} = 1.2 \times 10^{11}$ at injection, one to four batches of 72 bunches spaced 25 ns.

Fig. 1 shows I_{200} versus time for three cycles, acquired at 23:38H, 23:57H and 23:58H ($+n$ dips in the Fig. legend means that there were n RF voltage dips more than required for the number of batches injected. The RF voltages and the transverse tunes had been constant during the time of these acquisitions. However, the chromaticity had been tuned during this period, see Fig. 2. The I_{200} data was parametrised using the parameters listed in App. B. The data show that $L_{\mathrm{i,l}} \gg L_{\mathrm{i,r}}$. The value of L_{ef} for Fig. 1 (top) and for Fig. 1 (centre, bottom) differ by about 2 dB. There are at least two reasons for this difference. Firstly, the last two cases were acquired while four instead of three batches were injected (cleaning effect of injection kicker pulse). Secondly, the SPS had been tuned in between these measurements as already mentioned. The results for $L_{\mathrm{i,l}}$, $L_{\mathrm{i,r}}$ and L_{ef} for Fig. 1 (centre, bottom) are fairly equal. Both measurements were made shortly one after the other. All I_{200} measurement results are listed in Table D.1 (App. D).

3 2012-03-27

Using the same cycle, MD_26_L25200_2012x_V1 as 2012-03-26, more I_{200} measurements were made in the evening of 2012-03-27. Typical bunch intensity $N_{\mathrm{Q}} = 1.2 \times 10^{11}$ at injection, 72 bunches spaced 25 ns.

The 200 MHz RF voltage program consisted of segments of 2 MV at the time of the first four injections (not six as 2012-03-26) and 3 MV for the rest of the flat bottom if not stated otherwise. The 800 MHz RF system delivered a const. voltage of 350 kV.

The transverse tune and chromaticity settings were practically the same as at the end of the measurement series of 2012-03-26.

With these settings the data shown in Fig. 3 was acquired. Fig. 3 (top) shows an I_{200} measurement with TX6 tripped. Not surprisingly a fair amount of uncaptured beam can be seen. Fig. 3 (centre, bottom) shows two cases of two consecutive cycles acquired with all TX operational.

Between 20:18H and 21:40H a modified 200 MHz RF voltage programme was used. There were two extra voltage dips at times corresponding to the injection of the fifth and sixth batch. The TWC 800 MHz voltage still const. 350 kV. Acquisitions during that time are shown in Fig. 4 and Fig. 5.

Fig. 4 (bottom) and Fig. 5 show cases where the second batch was injected with a non-standard offset with respect to the first batch. The effect of uncaptured beam being confined between the two batches can be clearly seen (see also movie_491_571_3fps.avi).

The evolution of Q_{H}, Q_{V} and Q'_{V} during the time of the I_{200} measurements between 19:47H and 21:38H is shown in Fig. 6. Q'_{H} had not been changed during that time.

The values of $L_{\mathrm{i,l}}$ are similar to the one of 2012-03-26. There is a larger scatter for the $L_{\mathrm{i,r}}$ data which is between -61 dB and -65 dB. As 2012-03-26, with less batches injected the level L_{ef} increased. All I_{200} measurement results are listed in Table D.1 (App. D).

4 2012-03-28

The longitudinal quadrupole beam stability along the flat bottom had not been satisfactory 2012-03-27. In the morning of 2012-03-28 the longitudinal damper phase offset had been slightly adjusted which seemed to improve the beam stability along the flat bottom.

I_{200} measurements were first made with the LHCMD_25ns_2011_V1 cycle (ID: 643, Timing User: LHCFAST3) at around 11:21H, see Fig. 7. Typical bunch intensity $N_{\mathrm{Q}} = 1.2 \times 10^{11}$ at injection, 72 bunches spaced 25 ns.

The RF voltage programme consisted of four dips at 2.0 MV and an RF voltage of 3.0 MV otherwise along the flat bottom. The 800 MHz RF voltage was 350 kV constant along the flat bottom.

The value of $L_{\mathrm{i,l}}$ was similar to the ones of the MD_26_L25200_2012x_V1 cycle used 2012-03-26 and 2012-03-27. Also the value of $L_{\mathrm{i,r}}$ was comparable to the ones for the same cycle during the previous days. The value of L_{ef} could not be established. The flat bottom of the LHCMD_25ns_2011_V1 cycle was too short to obtain an equilibrium distribution of the uncaptured beam around the SPS circumference.

At 18:41H an I_{200} measurement was made with the MD_26_L25200_2012x_V1 cycle, see Fig. 8. The typical bunch intensity was still $N_{\mathrm{Q}} = 1.2 \times 10^{11}$ at injection, 72 bunches spaced 25 ns, see BCT screenshot Fig. 9.

The RF voltage programme consisted of two dips of 2.0 MV and an RF voltage of 3.0 MV otherwise along the flat bottom. The 800 MHz RF voltage was 350 kV constant along the flat bottom.

The value of $L_{\mathrm{i,l}}$ of -54 dB was similar to the ones obtained during previous measurements with the MD_26_L25200_2012x_V1 cycle 2012-03-26 and 2012-03-27. The value of $L_{\mathrm{i,r}}$ of -66 dB was better than previously observed. The value of L_{ef} of -66 dB was the best seen so far since 2012-03-26. One reason could have been that there were no extra voltage dips.

5 2012-03-29

The first measurements of 2012-03-29 were made with the MD_26_L25200_2012x_V1 cycle. Typical bunch intensity $N_{\mathrm{Q}} = 1.7 \times 10^{11}$ at injection, 72 bunches spaced 25 ns in one or two batches.

The 200 MHz RF voltage programme consisted of segments of 2 MV at the time of the first injection only (Fig. 10 (top)) or at both two injections (Fig. 10 (centre, bottom)) and 3 MV for the rest of the flat bottom if not stated otherwise. The 800 MHz RF system delivered a const. voltage of 350 kV.

An I_{200} measurement with a single batch and without a dip at the time of the second injection is shown in Fig. 10 (top). A measurement with a dip at the time of the second injection and with one batch injected is shown in Fig. 10 (centre).

With the same RF voltage programme but two batches injected see Fig. 10 (bottom).

With the high intensity beam the values of $L_{\mathrm{i,l}}$ increased by about 7 dB, while the $L_{\mathrm{i,r}}$ values stayed about the same. For L_{ef} no single batch case values were available for comparison. Also for the two batch case with no extra dip no comparison values were available for L_{ef}. With $L_{\mathrm{ef}} = -66$ dB it was fairly small and smaller than most of the other cases with two batches and the same cycle. In the one batch case L_{ef} was about -67 dB.

The next I_{200} measurement was made using the LHCMD_25ns_2011_V1 (ID: 643, Timing User: LHCFAST3) cycle, standard optics and with acceleration. Typical bunch intensity $N_{\mathrm{Q}} = 1.2 \times 10^{11}$ at injection, 72 bunches spaced 25 ns in one batch.

The 200 MHz RF voltage program was 2 MV at the time of the first injection and 3 MV for the rest of the flat bottom. The 800 MHz RF system delivered a const. voltage of 350 kV at flat bottom.

An I_{200} measurement with a single batch is shown in Fig. 11. The results were about the same as for the two batch case of 2012-03-28 (Fig. 8). As there was only one injection, Fig. 11 (top right) shows a stronger accumulation of uncaptured beam behind the batch at the end of the flat bottom than in the case of 2012-03-28.

6 2012-03-30

Measurements of I_{200} were made with the cycle MD_26_L25200_2012_Q20_V1 (ID: 1752, Timing User: LHCMD2, MMI Target: LHCMD3) and the cycle LHCMD_25ns_2011_V1 (ID: 643, Timing User: LHCFAST3).

During the morning the first measurement was made on the cycle MD_26_L25200_2012_Q20_V1 (Q20 optics, long flat bottom, no acceleration) at 11:25H, see Fig. 12. It was immediately followed by a measurement on the cycle LHCMD_25ns_2011_V1 (standard optics, with acceleration), see Fig. 13. The amount of beam piling up behind the batch at the end of the flat bottom, Fig. 12 (top right) was however larger than previously. For a comparison Fig. 12 (bottom right) shows the pile-up of uncaptured beam in the case of a long flat bottom cycle, measured at about 7 s after injection.

For the MD_26_L25200_2012_Q20_V1 cycle, the 200 MHz RF voltage program was 3.5 MV at the time of the first injection and 5.5 MV for the rest of the flat bottom. The 800 MHz RF system delivered a const. voltage of 525 kV at flat bottom.

For the LHCMD_25ns_2011_V1 cycle, the 200 MHz RF voltage program was 2.0 MV at the time of the first injection and 3.0 MV for the rest of the flat bottom. The 800 MHz RF system delivered a const. voltage of 350 kV at flat bottom.

In both cases the bunch intensity was $N_{\mathrm{Q}} = 1.2 \times 10^{11}$ at injection, one batch of 72 bunches spaced 25 ns.

The data for the MD_26_L25200_2012x cycle, Fig. 13, were similar to the ones acquired 2012-03-29, Fig. 11, see also Table D.1.

For the Q20 cycle, Fig. 12, $L_{\mathrm{i,l}}$ was better than for the typical LHCMD_25ns_2011 cycle and similar to the typical MD_26_L25200_2012x cycle. The value of $L_{\mathrm{i,r}}$ was comparable to the other Q26 cycles. The value of L_{ef} was only -68 dB, the lowest value seen during since 2012-03-26 including all cycles.

Although the I_{200} measurement frames where acquired at manually triggered intervals, Fig. 12 shows that the uncaptured beam is moving faster to the left than for the Q26 cycles, see Fig. 13, e.g. For a given $\Delta p/p$ the distance covered by unbunched beam, with RF off, should scale like η. The value of η in the two cases Q26 and Q20 differ by about 2.9 ($\eta_{\mathrm{Q26}} = 6.2 \times 10^{-4}$, $\eta_{\mathrm{Q20}} = 1.8 \times 10^{-3}$ at $p = 26$ GeV/c) whereas the distance covered in the same time differs by only about a factor of 1.8. As the RF was not off and the bucket heights in both cases were not the same, 4.0×10^{-3} in the Q20 case and 5.1×10^{-3} in the Q26 case. The missing factor is probably due the difference of the phase space trajectories outside the buckets.

At the beginning of the afternoon measurements were made again with the same Q26 optics cycle, MD_26_L25200_2012_Q20_V1, now with four batches of the 25 ns beam, see Fig. 14.

The values of $Q'_{\rm V}$ had intentionally been lowered during the second half of the flat bottom to render the beam unstable. This was done in the context of studying transverse e-cloud instabilities.

The 200 MHz RF voltage program was 3.5 MV at the time of the first injection and only 4.5 MV for the rest of the flat bottom, i.e. 1.0 MV lower than during the morning. The 800 MHz RF system delivered a const. voltage of 525 kV at flat bottom.

The value of $L_{\rm i,l}$ was fairly high and $L_{\rm i,r}$ was the highest seen so far, probably due to the low RF voltage along the flat bottom. This might also explain the large value for $L_{\rm ef}$ of -60 dB in contrast to the measurement of the morning shown in Fig. 12.

7 Round trip times

All the I_{200} measurements where one batch had been injected, were used to determine the time from injection until the wave of uncaptured beam, leaving the front of the batch hit the back of the batch, $T_{\rm hit}$. This is nearly the time to make a full SPS turn, apart from the time which corresponds to the width of the batch (1.8 μs). The observed $T_{\rm hit}$ data are listed in Table 1 in increasing order.

Cycle	Int.	$V_{\rm RF}$	η	$\Delta p/p$	$T_{\rm hit}$ [s]	Remarks
MD_26_L25200_2012_Q20	lo	V_2	1.8×10^{-3}	4.0×10^{-3}	4.3 ± 0.3	Fig. 12
MD_26_L25200_2012x	hi	V_1	6.2×10^{-4}	5.1×10^{-3}	6.3 ± 0.3	Fig. 10 (top)
MD_26_L25200_2012x	hi	V_1	6.2×10^{-4}	5.1×10^{-3}	6.3 ± 0.3	Fig. 10 (centre)
LHCMD_25ns_2011	lo	V_1	6.2×10^{-4}	5.1×10^{-3}	8.1 ± 0.3	Fig. 11
LHCMD_25ns_2011	lo	V_1	6.2×10^{-4}	5.1×10^{-3}	8.2 ± 0.3	Fig. 13

Table 1: Summary of $T_{\rm hit}$ measurements in order of increasing $T_{\rm hit}$. The column Cycle indicates the LSA name (shortened), Int. whether the bunch intensity had been low (lo) or high (hi), $V_{\rm RF}$ the RF voltage programme used (V_1: V_{200}: 3 MV + V_{800}: 350 kV, V_2: V_{200}: 5.5 MV + V_{800}: 535 kV), ignoring whether there had been one or several dips at injection times, η the phase slip factor, $\Delta p/p$ the bucket half height and $T_{\rm hit}$ as described in the text.

The ratio of $T_{\rm hit}$ for the Q26 low intensity case and the Q20 low intensity case is about 1.9 ± 0.2. This corresponds about to the inverse of the ratio of $\eta \times \Delta p/p$ for the two cases which is 2.3.

Without the knowledge of the momentum spread of the injected beam it is difficult to estimate the difference between the $T_{\rm hit}$ values for the high and low intensity case. One can only expect that $T_{\rm hit}$ is shorter for the the high intensity case than for the low intensity case as the longitudinal emittance usually increases with larger intensity. Here $T_{\rm hit}$ is about 25% shorter in the high intensity case with respect to the low intensity case.

8 Conclusions

The EXA spectrum analyser can be used to measure the amount of uncaptured beam at flat bottom. In all measurements the majority of the uncaptured beam drifts to the left with respect to $f_{\rm rev}$. The uncaptured beam did not pass the presence of a batch where the RF voltage is higher than during the rest of the circumference. That the RF voltage is higher had been measured separately (TWC 200 MHz cavity return voltage). It is linked to an imperfect beam loading compensation of the cavity voltage.

The cleaning effect of any injection kick after the first one has to be taken into account as well as beam loss. A low value of $L_{\rm ef}$ can be obtained by injection kicks, by beam loss or small capture loss at injection and along the flat bottom.

For the cycle with a short flat bottom of about 10 s the distribution of the uncaptured beam was not uniform around the SPS circumference. For the cycles with about twice the flat bottom length this had been the case.

The results of the uncaptured beam measurements are summarised in two simplified Tables, one for the low intensity case, Table 2 and one for the high intensity case, Table 3.

Table 2 shows that $L_{\mathrm{i,l}}$ was typically -54 dB for all cycles with the standard SPS optics. The scatter of the $L_{\mathrm{i,l}}$ is small with respect to the scatter of the $L_{\mathrm{i,r}}$ values. In general the L_{ef} are better the smaller the number of extra dips is.

Table 3 shows that $L_{\mathrm{i,l}}$ was about 5 dB worse than in the low intensity case. The values for $L_{\mathrm{i,r}}$ are in about the same ball park as for the low intensity case. Surprisingly the values for L_{ef} are not worse than for the the low intensity case.

		Injection		End FB	
		$L_{\mathrm{i,l}}$	$L_{\mathrm{i,r}}$	L_{ef}	
Cycle	N	[dB]	[dB]	[dB]	Remarks
LHCMD_25ns_2011	1	-54	-66		no equil.
LHCMD_25ns_2011	2	-53	-65		Fig. 7, +2 dips, no equil.
MD_26_L25200_2012x	2	-54	-66	-66	Fig. 8
MD_26_L25200_2012x	2	-55	-62	-64	+4 dips
MD_26_L25200_2012x	3	-55	-65	-66	+1 dip
MD_26_L25200_2012x	3	-55	-69	-63	Fig. 1, +3 dips
MD_26_L25200_2012x	4	-55	-68	-65	+2 dips
MD_26_L25200_2012_Q20	1	-56	-62	-68	Fig. 12
MD_26_L25200_2012_Q20	4	-53	-58	-60	Fig. 14

Table 2: Simplified summary of I_{200} measurements with the low intensity beam of typically $N_{\mathrm{Q}} = 1.2 \times 10^{11}$ at injection. For the Table legend see Table D.1 (App. D).

		Injection		End FB	
		$L_{\mathrm{i,l}}$	$L_{\mathrm{i,r}}$	L_{ef}	
Cycle	N	[dB]	[dB]	[dB]	Remarks
MD_26_L25200_2012x	1	-48	-66	-67	Fig. 10, +0/+1 dip
MD_26_L25200_2012x	2	-49	-67	-66	Fig. 10

Table 3: Simplified summary of I_{200} measurements with the high intensity beam of typically $N_{\mathrm{Q}} = 1.7 \times 10^{11}$ at injection. For the Table legend see Table D.1 (App. D).

The I_{200} data cannot be used directly to establish the amount of uncaptured beam, see App. C for details.

For the low intensity case the values for T_{hit} scale approximately as the inverse of $\eta \times \Delta p/p$.

References

[1] T. Bohl. LHC Beam at 26 GeV/c, Observations of 2003-08-13 (I). Note 2003-24, CERN, Geneva, August 2003.

[2] T. Bohl. LHC beam 26 GeV/c to 450 GeV/c, Observations of 2003-08-27 (I). Note 2004-27, CERN, Geneva, September 2004.

[3] T. Bohl. I-LHC Intermediate Beam at injection into the SPS. Observations of 2011-12-07. Note 2011-77, CERN, Geneva, December 2011.

A EXA acquisition details

The EXA Spectrum Analyzer AVG COUNT was set to 20.

The saving of an EXA Spectrum Analyzer trace was done by hand at a rate as constant as possible. However, the spectrum analyser did not always react at a constant rate due to internal processing. The trace file modification time stamp was recorded and used, in some cases, to estimate the true frame rate. Most of the avi movie files were created with a rate of 3 fps, although the actual rate was different.

B I_{200} parameters

To describe the I_{200} measurement the following parameters were used:

$\boldsymbol{L_{\mathrm{i,l}}}$ level of I_{200} outside the batch with respect to the value within the batch, measured in front of the batch shortly after injection

$\boldsymbol{L_{\mathrm{i,r}}}$ level of I_{200} outside the batch with respect to the value within the batch, measured in behind the batch shortly after injection

$\boldsymbol{L_{\mathrm{ef}}}$ average level of I_{200} outside the batch(es) with respect to the value within the batch(es), measured at the end of the flat bottom

The measurement error is typically ± 1 dB (estimated).

C I_{200} and the amount of uncaptured beam

The amount of uncaptured beam can not be directly obtained from I_{200} without further assumptions. The value of L_{ef} provides just the signal level at one frequency component of the unbunched beam while the distribution of the uncaptured beam is not known. It might even change as a function of time due to a change of $\Delta p/p$. In addition the amount of uncaptured beam lost out of the machine during the flat bottom is not known. It might not even be proportional to the amount of captured beam lost during the same time.

Assuming the same distribution for the uncaptured beam as for the captured beam, the amount of uncaptured beam can be estimated as a fraction of the total amount of particles as

$$\frac{10^{L_{\mathrm{ef}}/20}(1-N/11)}{10^{L_{\mathrm{ef}}/20}(1-N/11)+N/11}$$

where N is the number of batches present, each occupying about $1/11$ of the SPS circumference. For all cases shown, the amount of uncaptured beam would then be less than 0.8%.

D Detailed table of measurement results

Cycle	Day	Int.	N	Injection $L_{\mathrm{i,l}}$ [dB]	Injection $L_{\mathrm{i,r}}$ [dB]	End FB L_{ef} [dB]	Remarks
MD_26_L25200_2012x	26	lo	3	-55	-69	-63	Fig. 1, +3 dips
MD_26_L25200_2012x	26	lo	4	-54	-68	-65	Fig. 1, +2 dips
MD_26_L25200_2012x	26	lo	4	-56	-67	-65	Fig. 1, +2 dips
MD_26_L25200_2012x	27	lo	3	-55	-63	-50	Fig. 3, TX off
MD_26_L25200_2012x	27	lo	3	-55	-65	-67	Fig. 3, +1 dip
MD_26_L25200_2012x	27	lo	3	-55	-65	-65	Fig. 3, +1 dip
MD_26_L25200_2012x	27	lo	2	-55	-63	-63	Fig. 4, +4 dips
MD_26_L25200_2012x	27	lo	2	-55	-61	-64	Fig. 4, +4 dips
MD_26_L25200_2012x	27	lo	2	-55	-61	-65/-50	Fig. 4, large dBU
MD_26_L25200_2012x	27	lo	2	-56	-63	-64/-50	Fig. 5, large dBU
MD_26_L25200_2012x	27	lo	2	-57	-64	-64/-55	Fig. 5, large dBU
LHCMD_25ns_2011	28	lo	2	-53	-65		Fig. 7, +2 dips, no equil.
MD_26_L25200_2012x	28	lo	2	-54	-66	-66	Fig. 8
MD_26_L25200_2012x	29	hi	1	-48	-66	-67	Fig. 10
MD_26_L25200_2012x	29	hi	1	-48	-66	-67	Fig. 10, +1 dip
MD_26_L25200_2012x	29	hi	2	-49	-67	-66	Fig. 10
LHCMD_25ns_2011	29	lo	1	-53	-65		Fig. 11, no equil.
MD_26_L25200_2012_Q20	30	lo	1	-56	-62	-68	Fig. 12
LHCMD_25ns_2011	30	lo	1	-54	-67		Fig. 13, no equil.
MD_26_L25200_2012_Q20	30	lo	4	-53	-58	-60	Fig. 14

Table D.1: Summary of uncaptured beam measurements. All measurements in chronological order. The column Cycle indicates the LSA name (shortened), Day the day of the measurement (2012-03-), Int. the bunch intensity, whether it had been lo (1.2×10^{11}) or hi (1.7×10^{11}), N the effective number of batches injected (effective: a batch injected 60 ms before the start of acceleration can not contribute to the amount of unbunched beam during the flat bottom), L the level of I_{200} outside the batch with respect to the value within the batch (see App. B for details). Note that the LHCMD_25ns_2011 has a short flat bottom (10.9 s) and that the distribution of the uncaptured beam around the SPS circumference had not been in equilibrium at the time of the end of the flat bottom. Large dBU refers to injections with a non-standard injection bucket (BU).

Figures

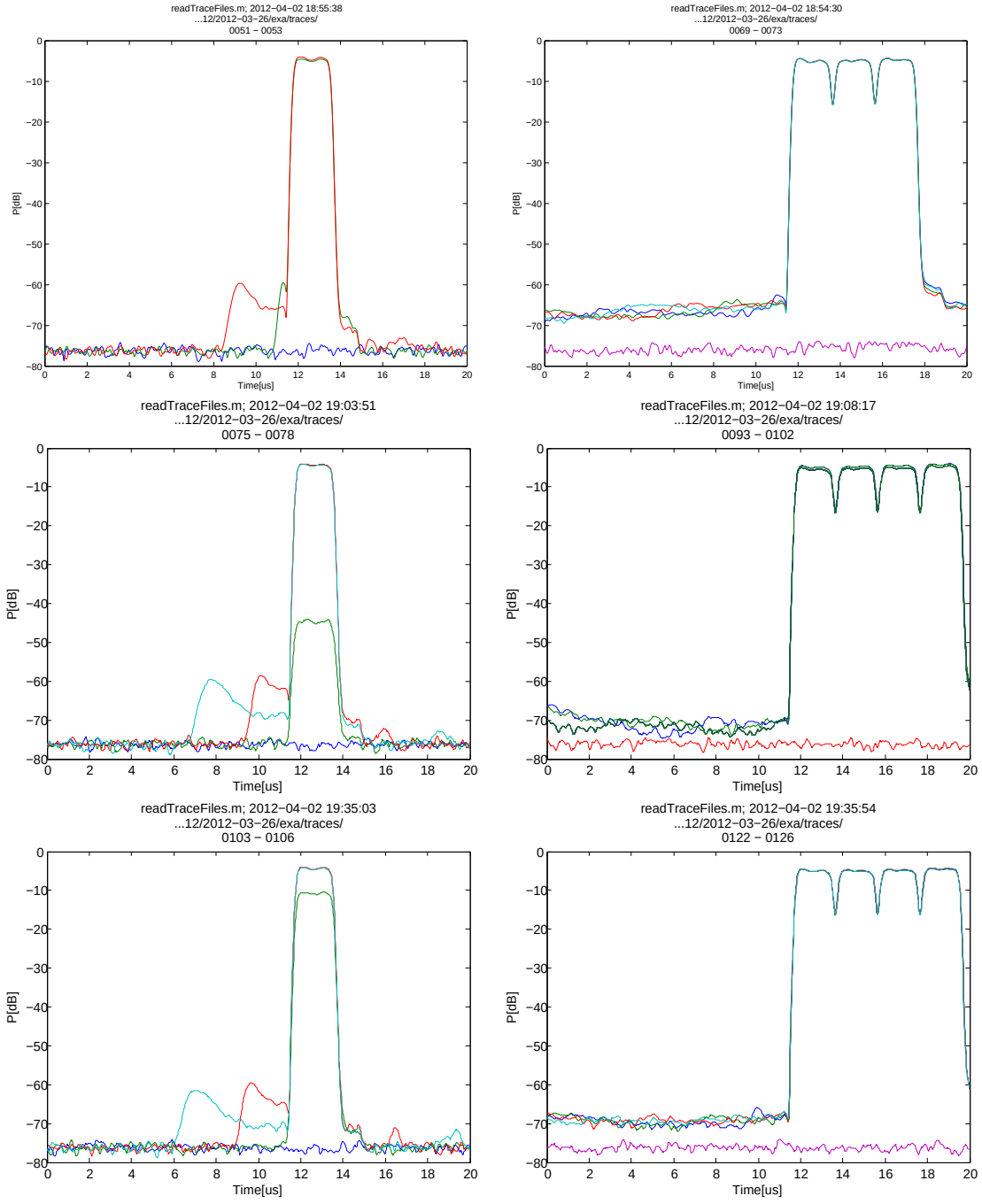

Figure 1: I_{200} versus time. Cycle MD_26_L25200_2012x_V1 (standard optics, long flat bottom, no acceleration). Left: at injection. Right: at end flat bottom. Top: three batches, +3 dips, 23:38H (movie_051_072_4fps.avi). Centre: four batches, +2 dips, 23:57H (movie_075_094_3fps.avi). Bottom: shortly afterwards, same conditions 23:58H (movie_103_125_3fps.avi). 2012-03-26.

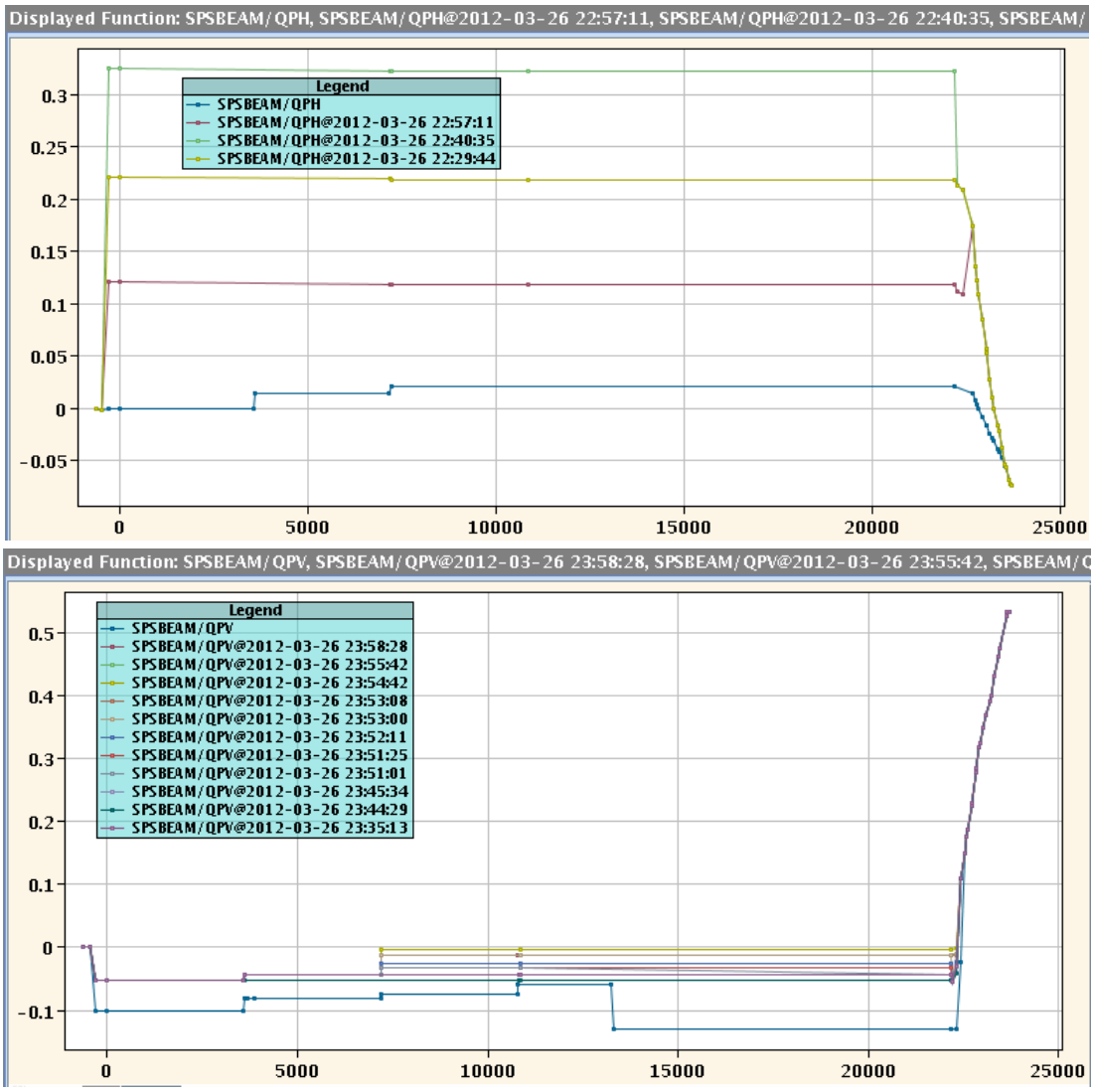

Figure 2: Chromaticity settings for the period when the data of Fig. 1 was acquired (23:38H to 23:58H). 2012-03-26. Cycle MD_26_L25200_2012x_V1.

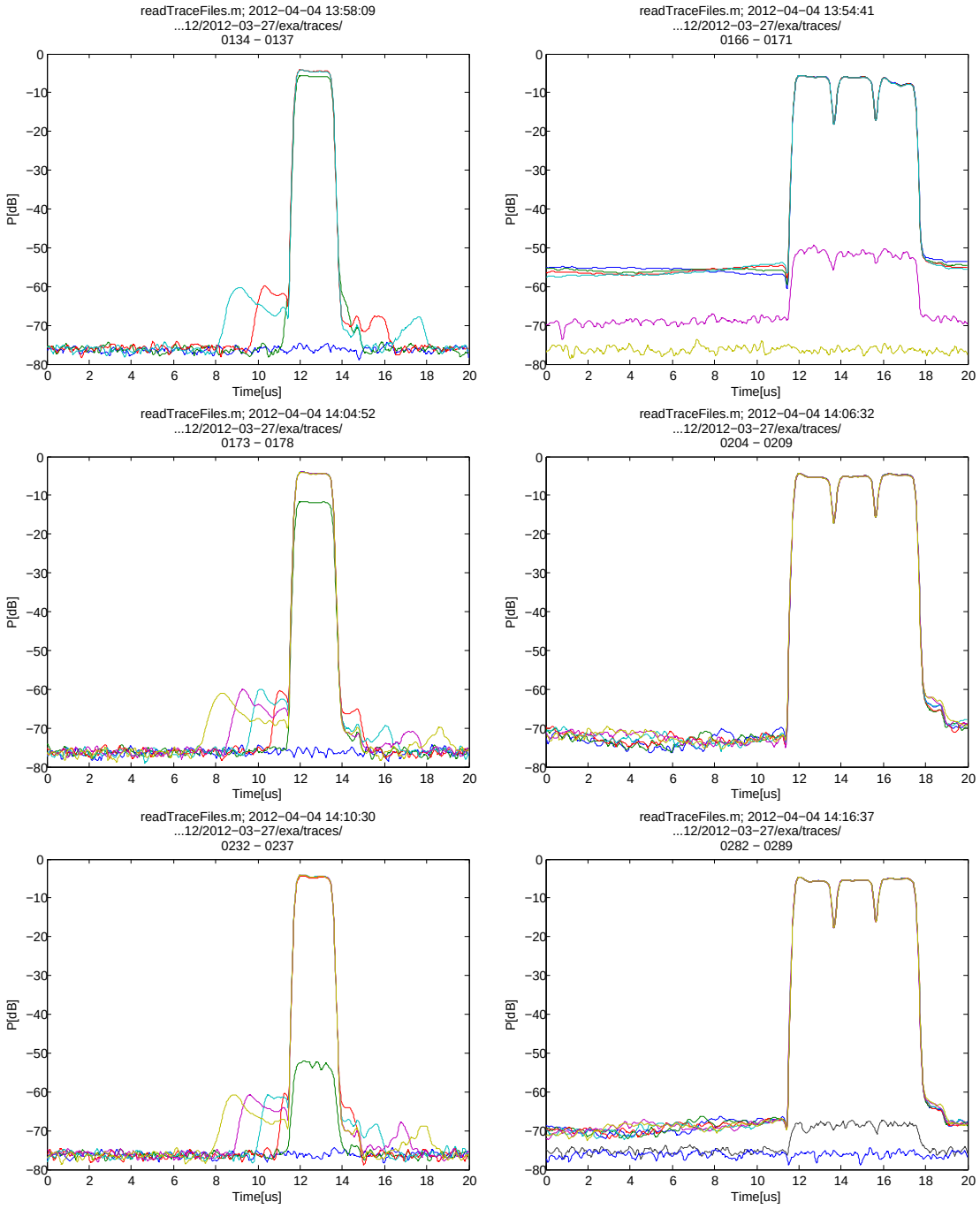

Figure 3: I_{200} versus time. Cycle MD_26_L25200_2012x_V1 (standard optics, long flat bottom, no acceleration). Left: at injection. Right: at end flat bottom. Top: 19:47H with TX6 tripped (movie_134_168_3fps.avi). With all TX working two further acquisitions were made. At 20:14H (centre) and shortly afterwards at 20:15H (bottom), see also movie_173_209_3fps.avi and movie_232_287_3fps.avi, respectively. 2012-03-27.

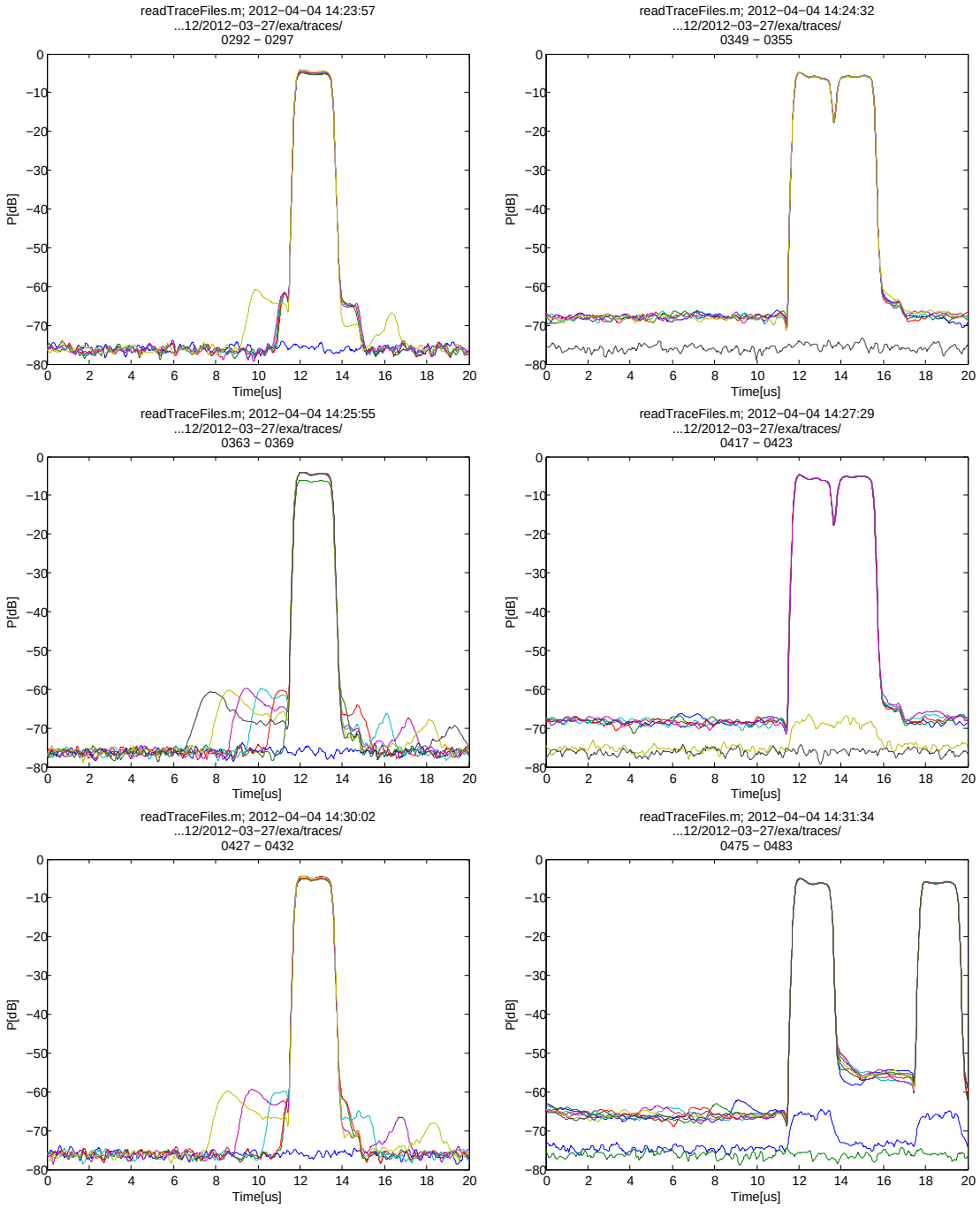

Figure 4: I_{200} versus time. Cycle MD_26_L25200_2012x_V1 (standard optics, long flat bottom, no acceleration). Left: at injection. Right: at end flat bottom. All three measurements with two extra 200 MHz RF voltage dips (see text). Top: 20:29H (movie_292_354_3fps.avi) Centre: 20:30H (movie_363_421_3fps.avi). Bottom: 21:05H (movie_427_481_3fps.avi). 2012-03-27.

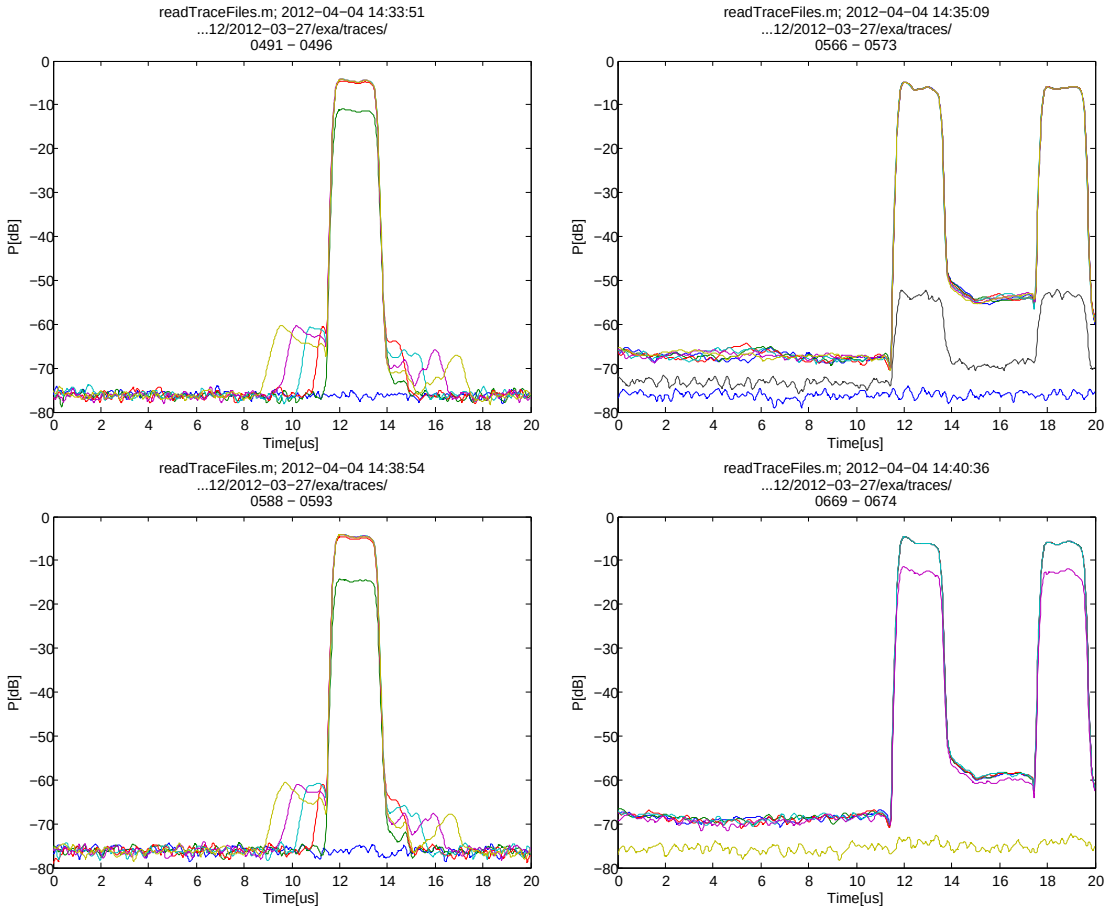

Figure 5: I_{200} versus time. Cycle MD_26_L25200_2012x_V1 (standard optics, long flat bottom, no acceleration). Left: at injection. Right: at end flat bottom. Both measurements with two extra 200 MHz RF voltage dips (see text). Top: 21:06H (movie_491_571_3fps.avi). Bottom: 21:38H (movie_588_673_3fps.avi). 2012-03-27.

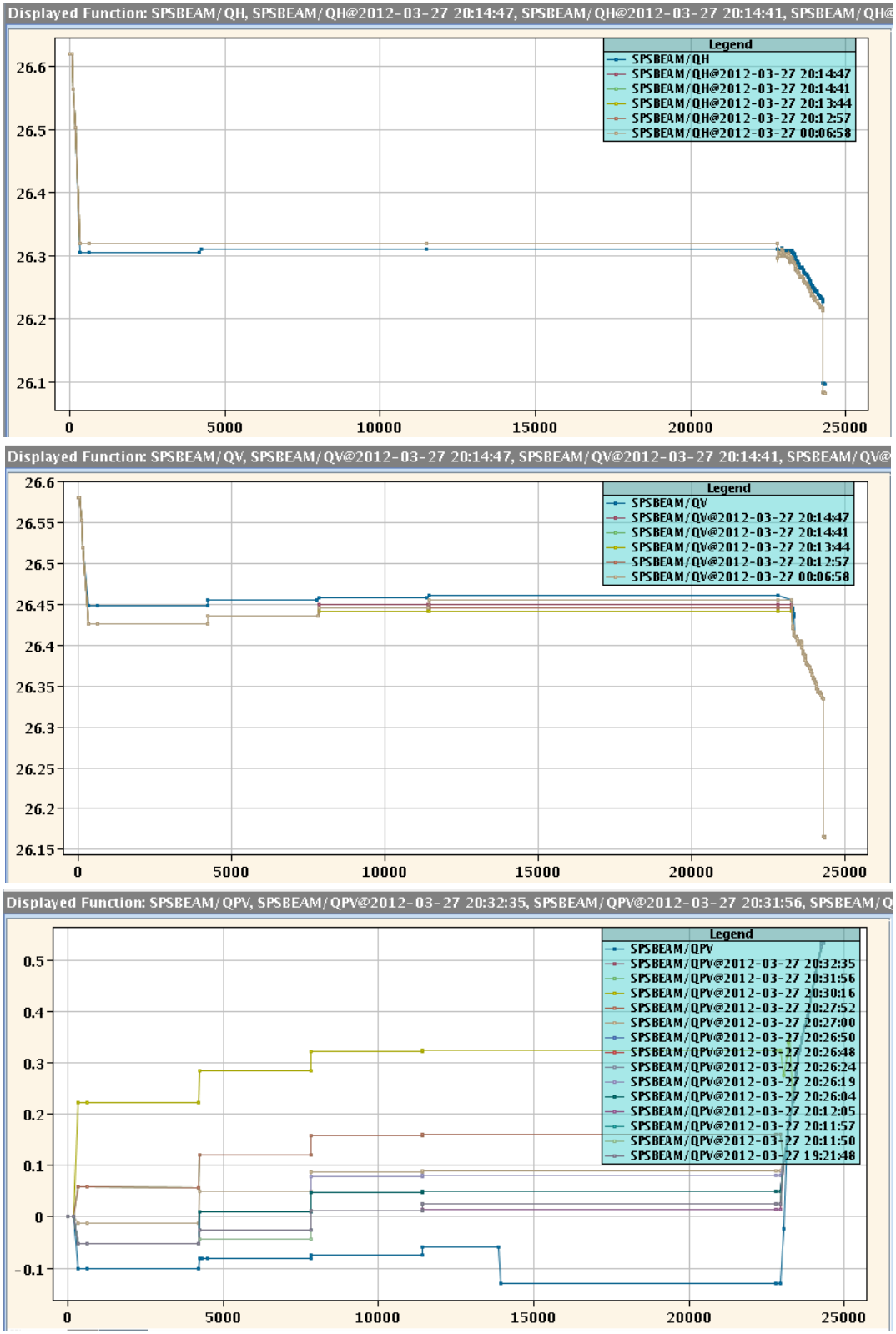

Figure 6: Evolution of Q_{H}, Q_{V} and Q'_{V} during the time of the I_{200} measurements between 19:47H and 21:38H, 2012-03-27. Q'_{H} had not been changed during that time.

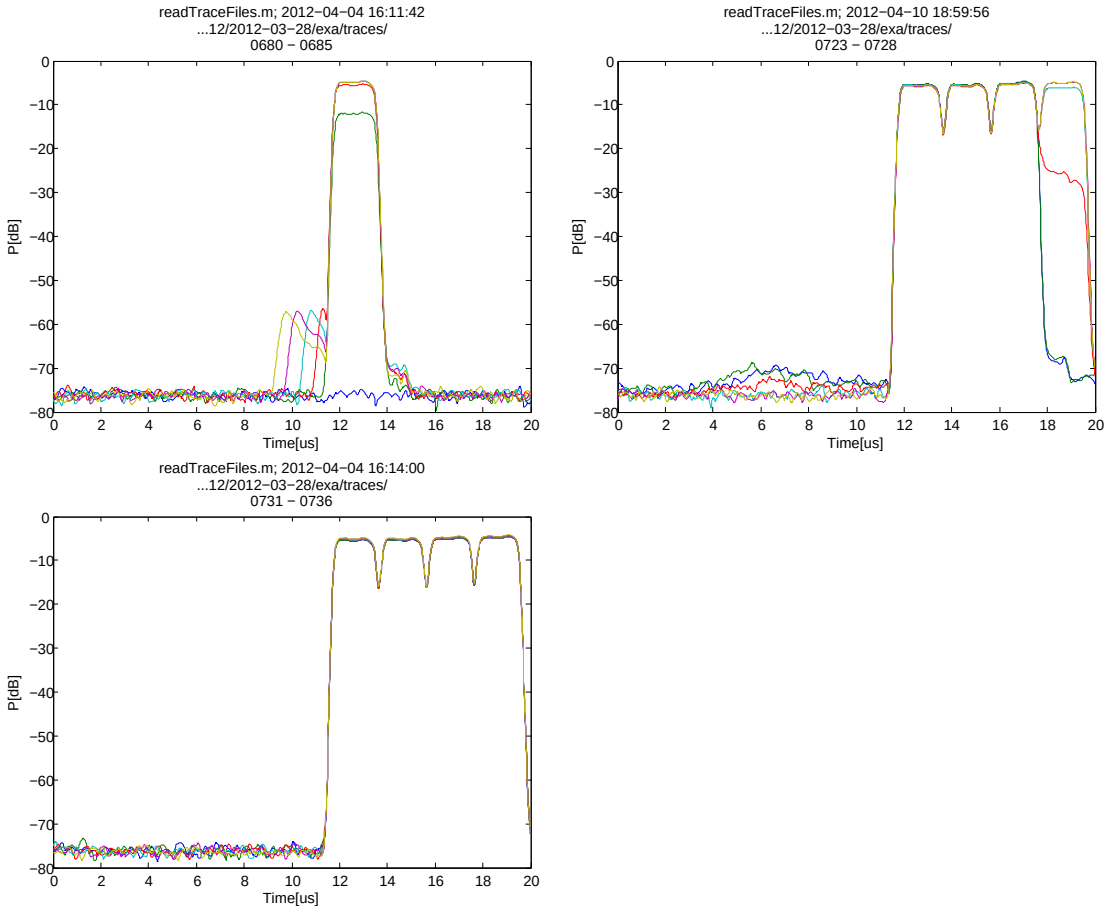

Figure 7: I_{200} versus time. Top left: at injection. Top right: at end flat bottom. Bottom: towards end of acceleration ramp. LHCMD_25ns_2011_V1 cycle (standard optics, short flat bottom). No equilibrium distribution of uncaptured beam to determine L_{ef}. movie_0747_0821_3fps.avi. 11:21H, 2012-03-28.

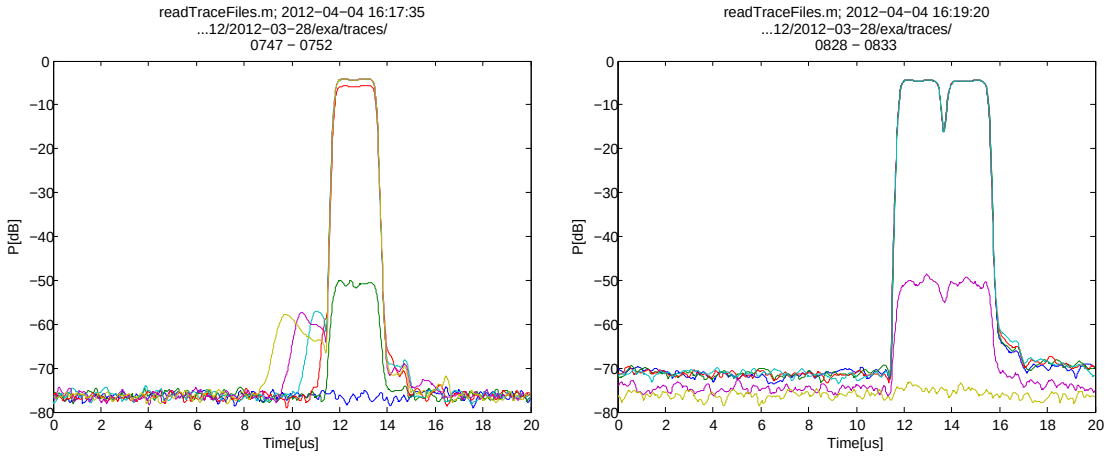

Figure 8: I_{200} versus time. Left: at injection, right: at end flat bottom. MD_26_L25200_2012x_V1 cycle (standard optics, long flat bottom, no acceleration). 18:41H. 2012-03-28.

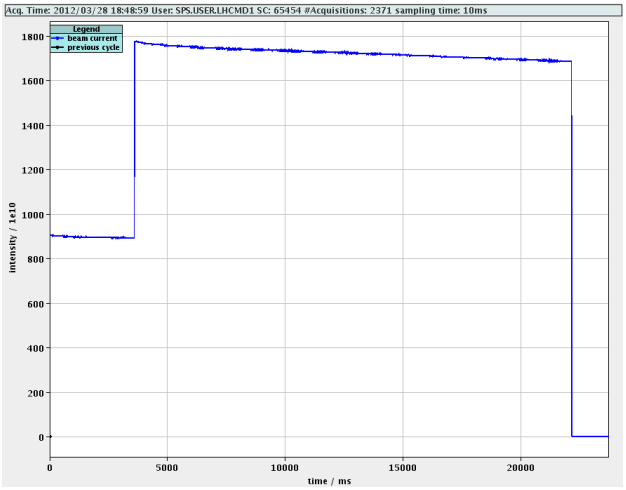

Figure 9: BCT screenshot LHCMD1. MD_26_L25200_2012x_V1 cycle (standard optics, long flat bottom, no acceleration). Acquired at about the same time as data of Fig. 8. 18:48H, 2012-03-28.

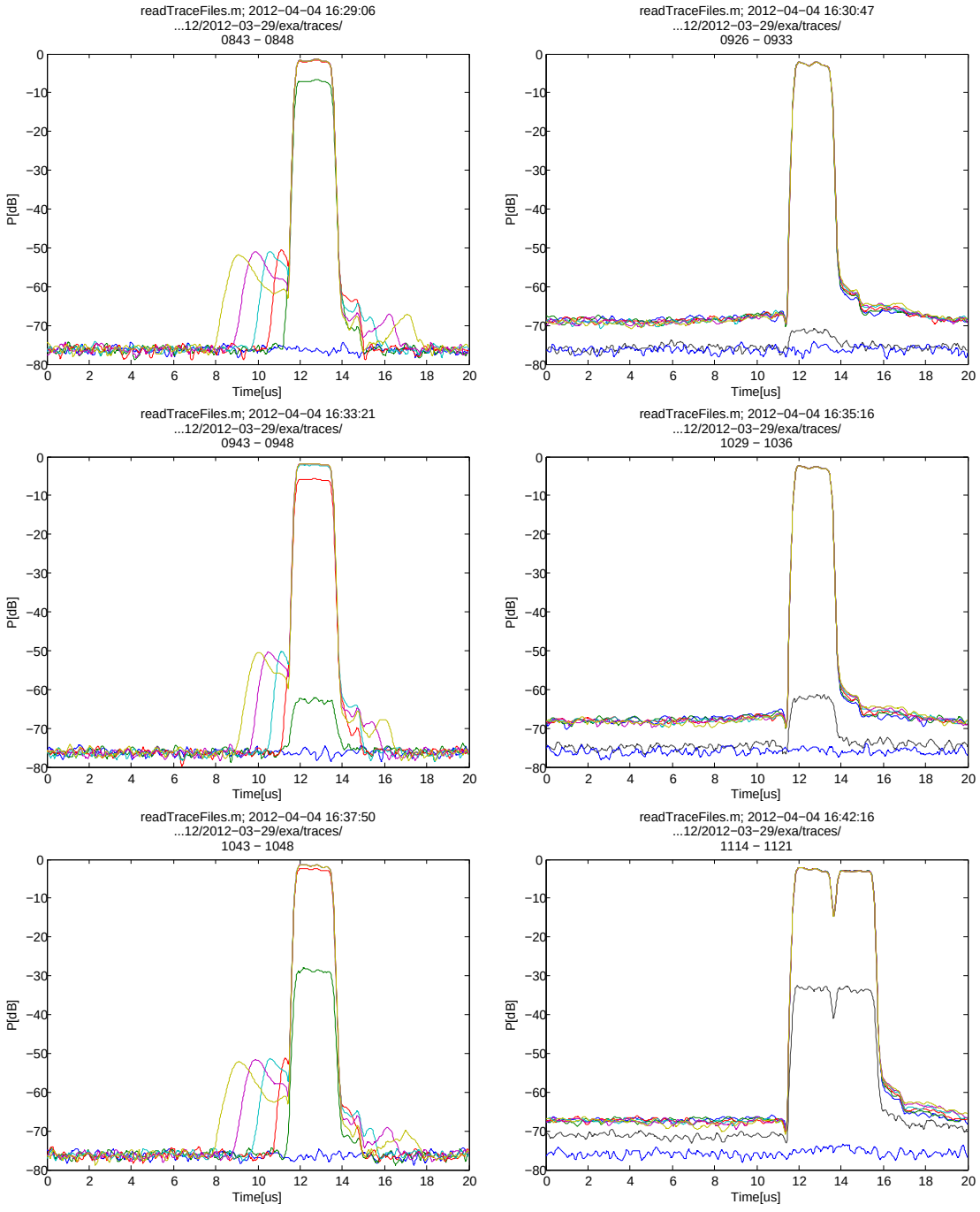

Figure 10: I_{200} versus time. MD_26_L25200_2012x_V1 cycle (standard optics, long flat bottom, no acceleration), $N_Q = 1.7 \times 10^{11}$ at injection. Left: at injection. Right: at end flat bottom. Top: with no RF voltage dip at the time of the second injection, 11:26H (movie_0843_0900_3fps.avi). Centre: with an RF voltage dip at the time of the second injection, 11:29H (movie_0943_1034_3fps.avi). Bottom: case of two batches and same voltage programme as for centre panels, 12:12H (movie_1043_1119_3fps.avi). 2012-03-29.

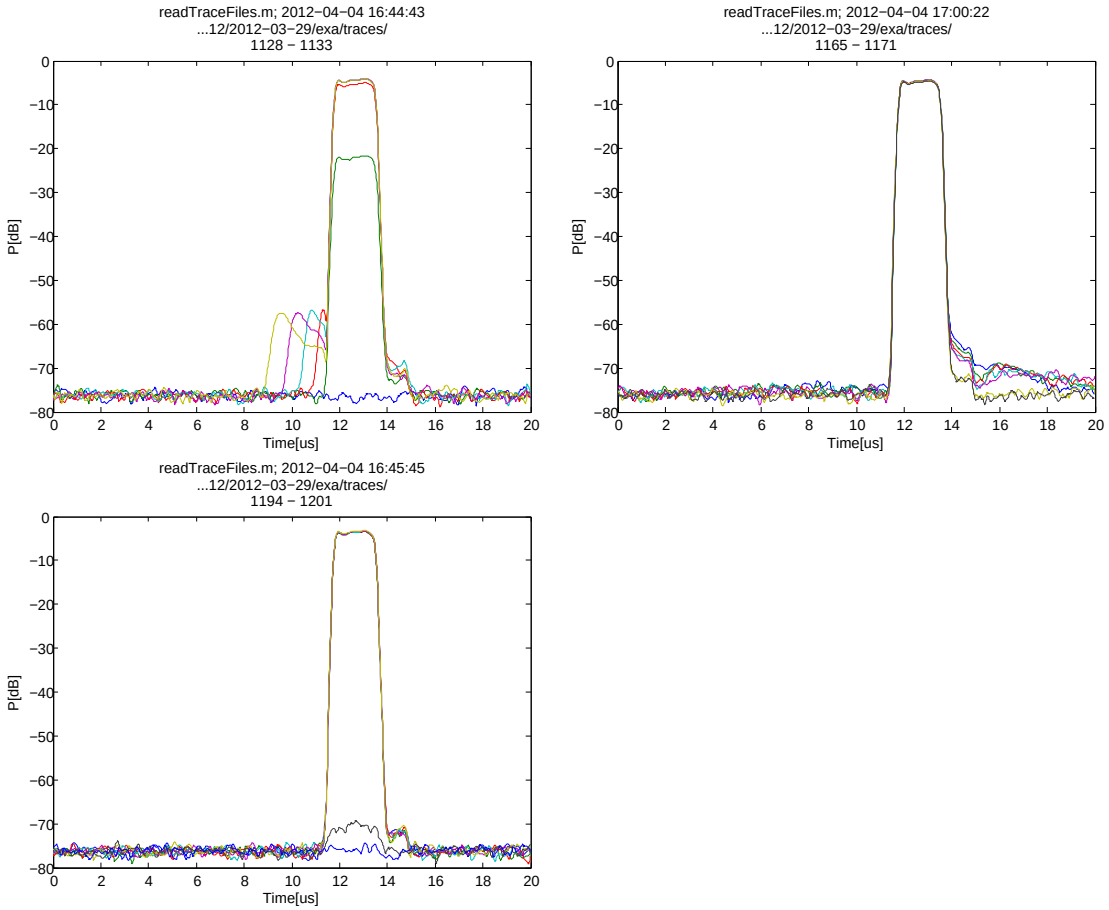

Figure 11: I_{200} versus time. LHCMD_25ns_2011_V1 cycle (standard optics, short flat bottom), $N_{\mathrm{Q}} = 1.2 \times 10^{11}$ at injection. Top left: injection. Top right: end flat bottom. The last two trances (top right) show the 200 MHz beam current early in the acceleration ramp. The major change of the 200 MHz beam current occurs at the beginning of acceleration during the about 4 μs behind the batch (14 $\mu\mathrm{s} \leqslant t \leqslant 19$ μs). Bottom: acceleration and flat top. movie_1128_1199_3fps.avi. 13:27H, 2012-03-29.

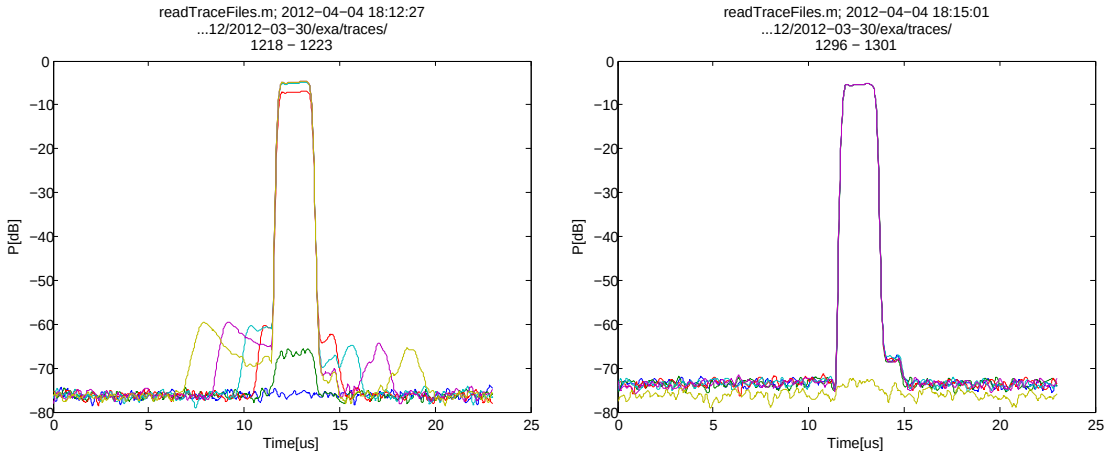

Figure 12: I_{200} versus time. Cycle: MD_26_L25200_2012_Q20_V1 (Q20 optics, long flat bottom, no acceleration). $N_{\mathrm{Q}} = 1.2 \times 10^{11}$ at injection. Left: injection, right: end flat bottom. movie_1218_1300_3fps.avi, frame rate determined from time stamps about 3.6 fps. 11:24H. 2012-03-30.

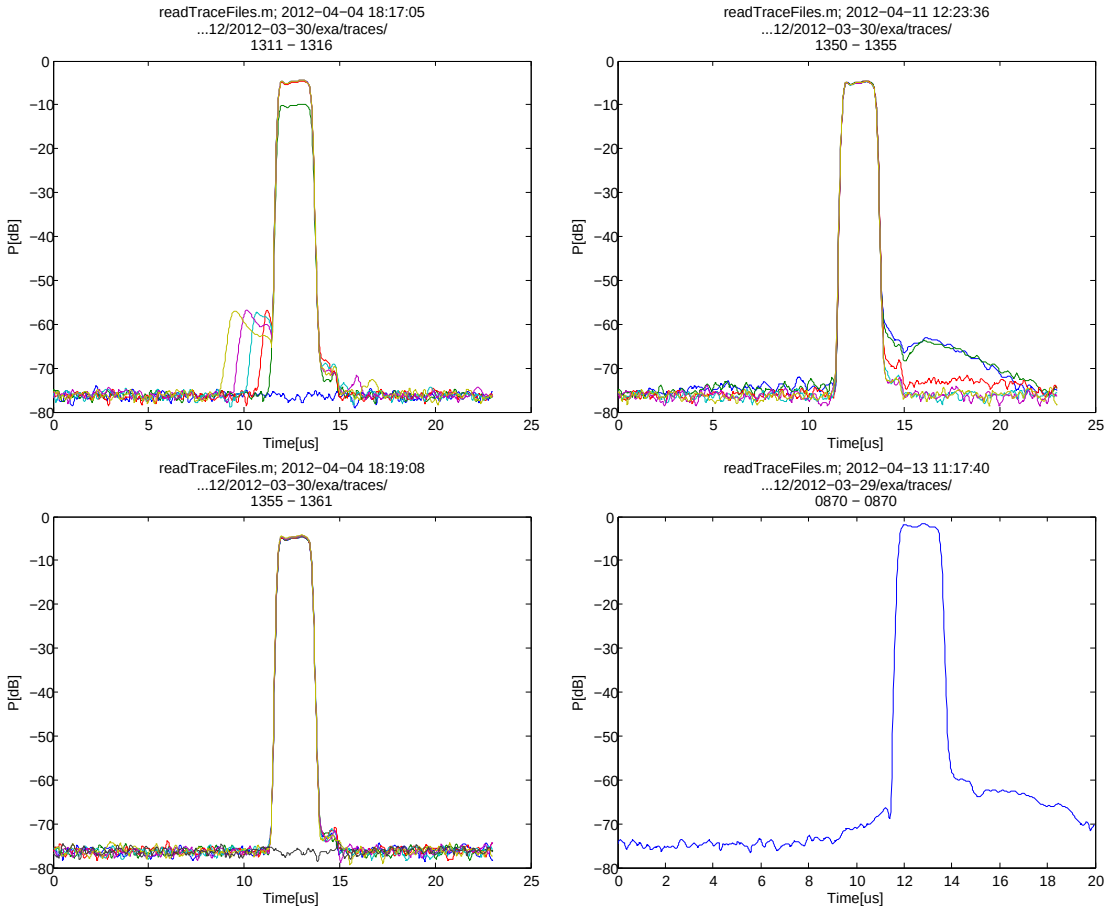

Figure 13: I_{200} versus time. Cycle: LHCMD_25ns_2011_V1 (standard optics, short flat bottom). $N_{\mathrm{Q}} = 1.2 \times 10^{11}$ at injection. Top left: injection. Top right: end flat bottom. Bottom left: end of acceleration ramp. movie_1311_1360_3fps.avi, frame rate determined from time stamps about 4.0 fps. 11:25H, 2012-03-30. The pile-up of uncaptured beam behind the batch at about 10 s after injection (top right) is similar to the one observed with the MD_26_L25200_2012x_V1 cycle (bottom right), acquired 11:26H, 2012-03-29, see Fig. 10 (top). The pile-up is also similar to the one in Fig. 11 (top right).

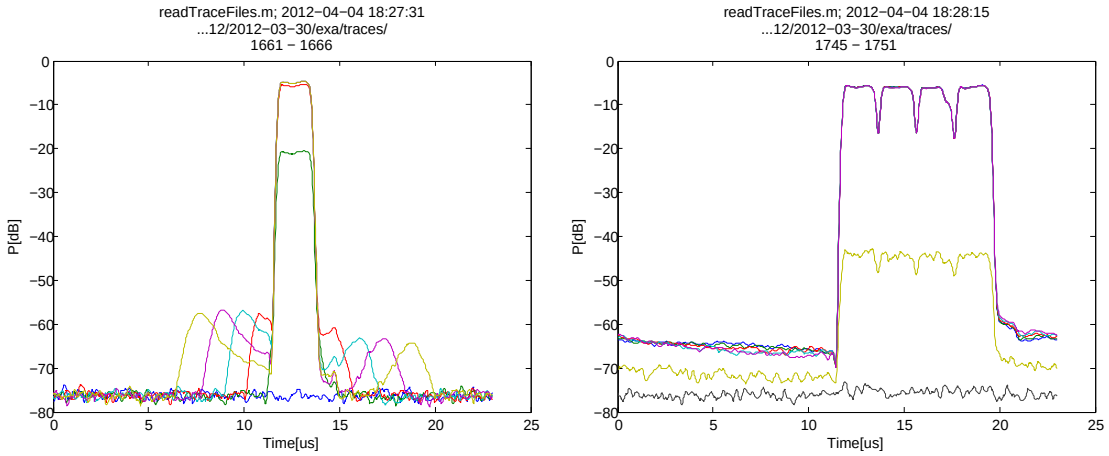

Figure 14: I_{200} versus time. Left: injection, right: end flat bottom. Cycle: MD_26_L25200_2012_Q20_V1 (Q20 optics, long flat bottom, no acceleration). $N_{\mathrm{Q}} = 1.2 \times 10^{11}$ at injection. movie_1661_1749.avi. 14:30H. 2012-03-30.